C Journal of Carbon Research

MDPI

Article

Study of the Influence of Silicon-Containing Diamond-like Carbon Coatings on the Wear Resistance of SiAlON Tool Ceramics

Marina A. Volosova * and Anna A. Okunkova

Department of High-Efficiency Processing Technologies, Moscow State University of Technology STANKIN, Vadkovskiy per. 3A, 127055 Moscow, Russia

* Correspondence: m.volosova@stankin.ru; Tel.: +7-499-972-94-29

Abstract: DLC coatings have low adhesive bond strength with the substrate and a high level of residual stresses. This paper is devoted to researching a complex of characteristics of a DLC-Si coating deposited on samples of SiAlON ceramics with intermediate coatings (CrAlSi)N pre-formed to improve the adhesive bond strength employing vacuum-plasma spraying. DLC-Si coatings were formed by chemical vapor deposition in a gas mixture of acetylene, argon, and tetramethylsilane supplied through a multichannel gas purge system controlling the tetramethylsilane volume by 1, 4, 7, and 10%. The SiAlON samples with deposited (CrAlSi)N/DLC-Si coatings with different silicon content in the DLC layer were subjected to XPS and EDX analyses. Tribological tests were carried out under conditions of high-temperature heating at 800C. The nanohardness and elasticity modulus of the rational (CrAlSi)N/DLC-Si coating with Si-content of 4.1% wt. were 26 ± 1.5 GPa and 238 ± 6 GPa, correspondingly. The rational composition of (CrAlSi)N/DLC-Si coating was deposited on cutters made of SiAlON ceramics and tested in high-speed machining of aircraft nickel-chromium alloy compared to uncoated and DLC-coated samples. The average operating time (wear resistance) of (CrAlSi)N/DLC-Si(4.1% wt.)-coated end mills before reaching the accepted failure criterion was 15.5 min when it was 10.5 min for the original cutters.

Keywords: ceramic cutters; cutting ceramics; coefficient of friction; (CrAlSi)N sublayer; DLC-Si coatings; high-temperature wear; SiAlON; sp3- and sp2-hybridizations; wear resistance

Citation: Volosova, M.A.; Okunkova, A.A. Study of the Influence of Silicon-Containing Diamond-like Carbon Coatings on the Wear Resistance of SiAlON Tool Ceramics. *C* **2023**, *9*, 50. https://doi.org/10.3390/c9020050

Academic Editor: Gil Gonçalves

Received: 22 February 2023
Revised: 3 May 2023
Accepted: 9 May 2023
Published: 16 May 2023

1. Introduction

Nowadays, diamond-like carbon (DLC) coatings are widely used in mechanical engineering as wear-resistant layers, the primary function of which is to increase the hardness significantly and reduce the coefficient of the friction of the product's working surfaces during machining under various contact loads and intense frictional interaction of counter bodies with various materials [1–5]. DLC coatings consist of carbon atoms with sp^3- and sp^2-hybridizations combined into an amorphous structure. The high content of carbon atoms with diamond sp^3-bonds in the presence of graphite-like sp^2-bonds provides a unique set of parameters for coatings of this type [6–9].

DLC coatings have apparent positive features but many disadvantages at the same time. For example, the majority of the diamond-like carbon coatings including both hydrogen-free (a-C) and hydrogenated (a-C:H) have low adhesive bond strength with the substrate and a high level of residual stresses, which are aggravated by increasing DLC coatings' thickness [10–14]. In addition, a significant limitation of the coatings' application areas is related to their relatively low thermal stability, which results in the coatings rapidly losing their properties under conditions of exposure to high thermal loads on the contact surfaces [15,16].

Various technological approaches have become widespread among the leading research groups to minimize these shortcomings. The most effective is alloying with various elements during the DLC coating formation. For example, introducing metal and metalloid atoms into a diamond-like carbon matrix can significantly reduce internal stresses and improve

coatings' mechanical and tribological properties since DLC coatings have a high hardness and low friction coefficient when alloying elements are characterized by high ductility. In addition, introducing additional elements can increase the operation efficiency of DLC coatings under thermal loads due to the thermally stable oxides' formation upon heating [17–19]. Another technological approach that has proved its advantages in practice is the formation of intermediate coatings before DLC coating's deposition to increase the total thickness of the coating while ensuring the high strength of the adhesive bond with the substrate [20–23]. In addition, the intermediate coating can protect the product's contact surfaces from premature wear for an additional time after the abrasion of the outer DLC layer.

There is no universal technological solution with relatively intensive development of improving DLC coatings. Moreover, one must proceed from the specific operating conditions of the product (substrate) on which the coating is applied and pay special attention to the type and substrate properties to develop a DLC coating and its deposition technique. Evaluation of the effectiveness of the chosen approach to the DLC coating formation should be carried out under thermomechanical loads corresponding to the nature and level of operational ones [24,25].

DLC coatings' deposition on metal and metal-ceramic alloys is a reasonably well-studied area, but the deposition of these coatings on ceramics remains outside the main focus of research groups. Technical ceramics are structurally inhomogeneous composite materials with high hardness and heat resistance, products which are operated under the simultaneous action of large mechanical and thermal loads in many cases [26–30]. The influence of various thin-film coatings based on nitrides of refractory metals on the wear resistance of ceramics has been studied by various authors [31–34]. The results of studies of the potential possibilities of using DLC coatings to improve the wear resistance of ceramic products are in areas of scientific and practical interest. Preliminary studies performed by the authors of this work have shown that the formation of intermediate coatings, in particular, multicomponent nitride such as (CrAlSi)N before DLC coatings' deposition, as well as doping of the outer DLC coating of silicon, is an approach that has a particular potential and needs more in-depth study [35–39].

One of the most modern SiAlON ceramics, which exhibit improved physical and mechanical properties among industrially produced ceramic materials and is used to manufacture various types of metalworking ceramic tools, was chosen as substrates for DLC coatings' deposition [39–44]. At the same time, end mills designed for high-speed machining aviation-type nickel-chromium alloys, the so-called superalloys, are of particular practical interest among tools made from SiAlON.

Thus, among their various advantages, DLC-coatings exhibit a low level of adhesion to the ceramic substrate and a high level of stress. These shortcomings only increase with increasing coating thickness and ultimately affect the durability of the cutting tool, which is especially important in the high-temperature machining of nickel-containing alloys.

This work is aimed at solving this problem and proposes an original integrated approach to improve the tool-life parameters, namely to use the method of alloying the DLC-coating deposited by a chemical method and the formation of an intermediate coating to improve the adhesive bond.

Namely, the study is devoted to the research of the effect of DLC coatings with different silicon contents formed by chemical vapor deposition on the wear resistance of SiAlON tool ceramics where DLC-Si was deposited on a preformed (CrAlSi)N intermediate coating. The volume content of tetramethylsilane in the gas mixture was varied at the level of 1, 4, 7, and 10% vol. to provide different content of the alloying element in DLC-Si. The (CrAlSi)N/DLC-Si coatings were subjected to XPS and EDX analyses, nanohardness and elastic modulus measurements, as well as tribological tests at high-temperature friction sliding. The rational composition of the (CrAlSi)N/DLC-Si coating (from the point of view of high-temperature tribological tests' results, in other words, the coating option that has shown the best results in tests) was deposited on end-mill samples made of SiAlON tool ceramics, which were tested during high-speed machining of aircraft NiCr20TiAl nickel-

chromium alloy. During testing, data were obtained on wear resistance and prospects for further application of these coatings.

2. Materials and Methods

2.1. Characteristics of SiAlON-Ceramic Substrates and End Mills Made of It

When conducting research, SiAlON-based ceramics for tool purposes was used as a substrate material for (CrAlSi)N/DLC-Si coating. It has the following physical and mechanical properties: hardness of 15.0 GPa; density of 3.45 g/cm^3; bend strength of 870 MPa; Young's modulus of 280 GPa; fracture toughness K_{1c} of 6.9 MPa·m$^{1/2}$. The technology of high-speed spark plasma sintering of the initial ceramic powders α-SiAlON and β-SiAlON was used to obtain samples based on SiAlON under the conditions of the appearance of spark plasma between the particles of the sintered workpiece and the passage of pulsed currents through it [35].

Figure 1a shows the SEM image of the microstructure of samples of sintered SiAlON ceramics obtained on a Tescan VEGA 3 LMH scanning electron microscope (Brno, Czech Republic). Samples in the form of washers of 19 mm in diameter and 7 mm in height were made from sintered ceramic blanks, which were subsequently coated with (CrAlSi)N/DLC-Si compositions for various types of analysis and tribological tests. In addition, samples of end mills with a diameter of 10 mm and a length of 60 mm were made from sintered ceramic blanks. An SEM image of its cutting part is shown in Figure 1b. A photograph of their general view is presented in Figure 1c. The technology of diamond sharpening of end mills is described in detail in [35]. (CrAlSi)N/DLC-Si coatings were deposited on the end mills, which showed the best performance in high-temperature tribological tests.

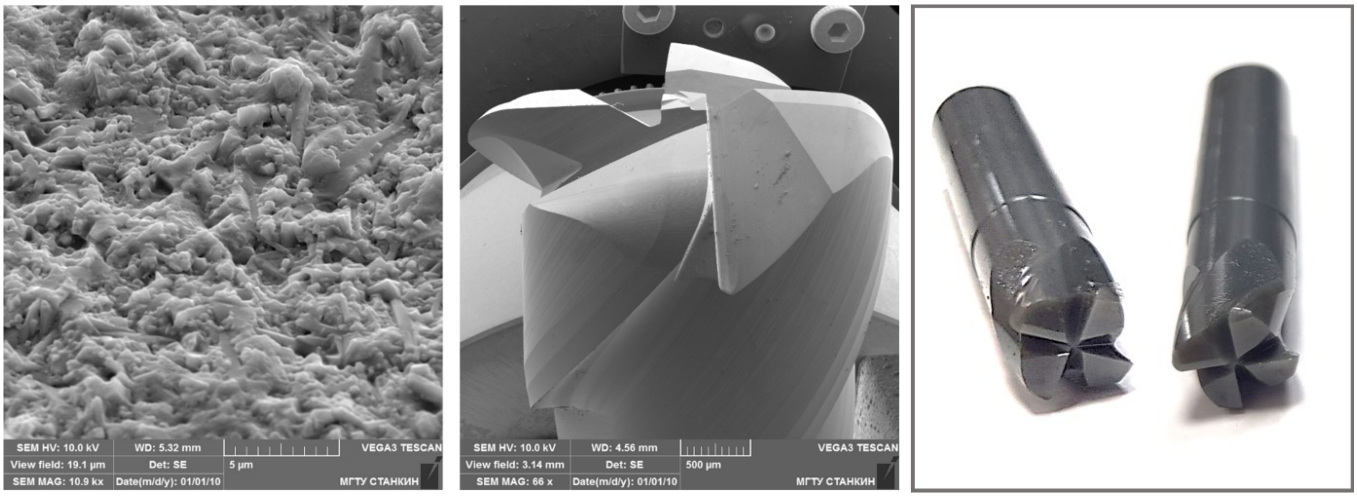

(**a**) (**b**) (**c**)

Figure 1. SEM images of the microstructure of SiAlON ceramics (**a**), the cutting part of the end mill made from it (**b**) and a general view of the ceramic end mills (**c**).

The X-ray diffraction pattern of a sintered sample made of SiAlON ceramics used in the research is shown in Figure 2. X-ray phase analysis was carried out on a Bruker D8 Advance diffractometer (Bruker AXS GmbH, Karlsruhe, Germany) with monochromatic CuKα radiation when shooting in the angle range of 20–90° 2Θ with a step of 0.05° and exposure to each point for 5 s. The analysis of the obtained results using the ICDD PDF-2 database made it possible to reveal the main structural components of the sintered SiAlON ceramics, which is represented by the Si_5AlON_7 and Si_3N_4 phases.

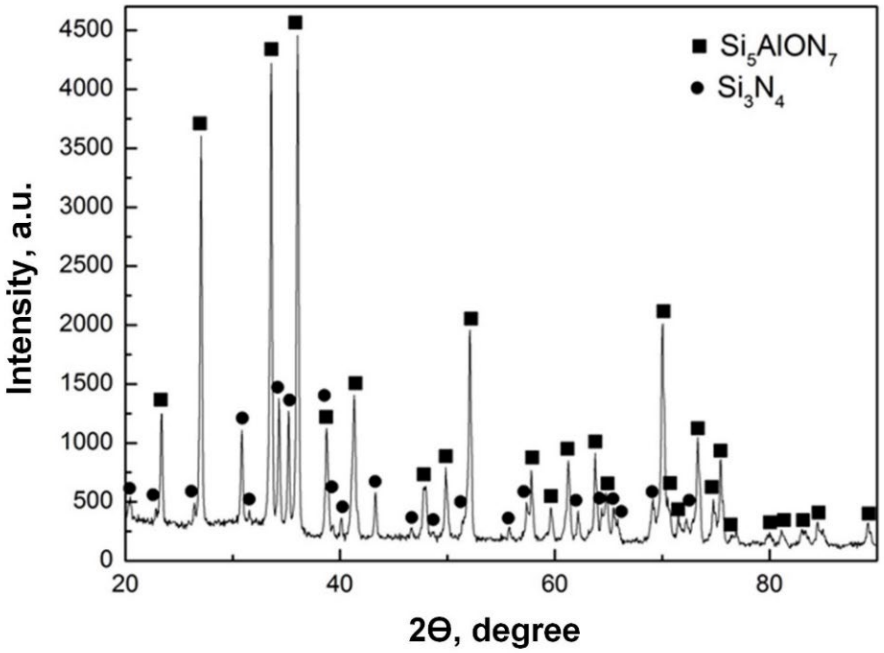

Figure 2. X-ray diffraction pattern of a sample made of SiAlON ceramics used in research.

2.2. (CrAlSi)N/DLC-Si Coating Technique for SiAlON-Ceramic Samples

Coating of SiAlON-ceramic samples was carried out on an experimental and industrial technological unit developed at Moscow State University of Technology STANKIN (Moscow, Russia), equipped with a vacuum-arc discharge plasma generation device for the deposition of a nitride transition nitride coating (CrAlSi)N by evaporation of AlSi and Cr cathodes, a multichannel system gas inlet and glow discharge generation system, which ensures the formation of a coating based on DLC layers by gas-phase deposition in glow discharge plasma through a chemical reaction and decomposition of the components of a gas mixture of acetylene, argon, and tetramethylsilane. The original unit is based on a set of solutions created by the research group of the university and allows the deposition of a wide range of transition coatings based on refractory metal nitrides [45–49]. The implemented-in-the-unit DLC deposition technique is similar to the approach developed and implemented by PLATIT (Selzach, Switzerland).

The general view and internal design of the processing unit used for the deposition of CrAlSi)N/DLC-Si coatings are shown in Figure 3. The volume content of tetramethylsilane in the gas mixture was varied in the volume of 1, 4, 7, and 10% to provide different content of the alloying element (silicon) in DLC-Si composition. The total thickness of the deposited coatings was controlled by the deposition time and amounted to ~3.9 μm including ~1.9 μm for (CrAlSi)N and ~2.0 μm for DLC. A block diagram of the technological process and the sequence of operations with the modes of (CrAlSi)N/DLC-Si coating deposition on samples made of SiAlON ceramics is shown in Figure A1 (Appendix A).

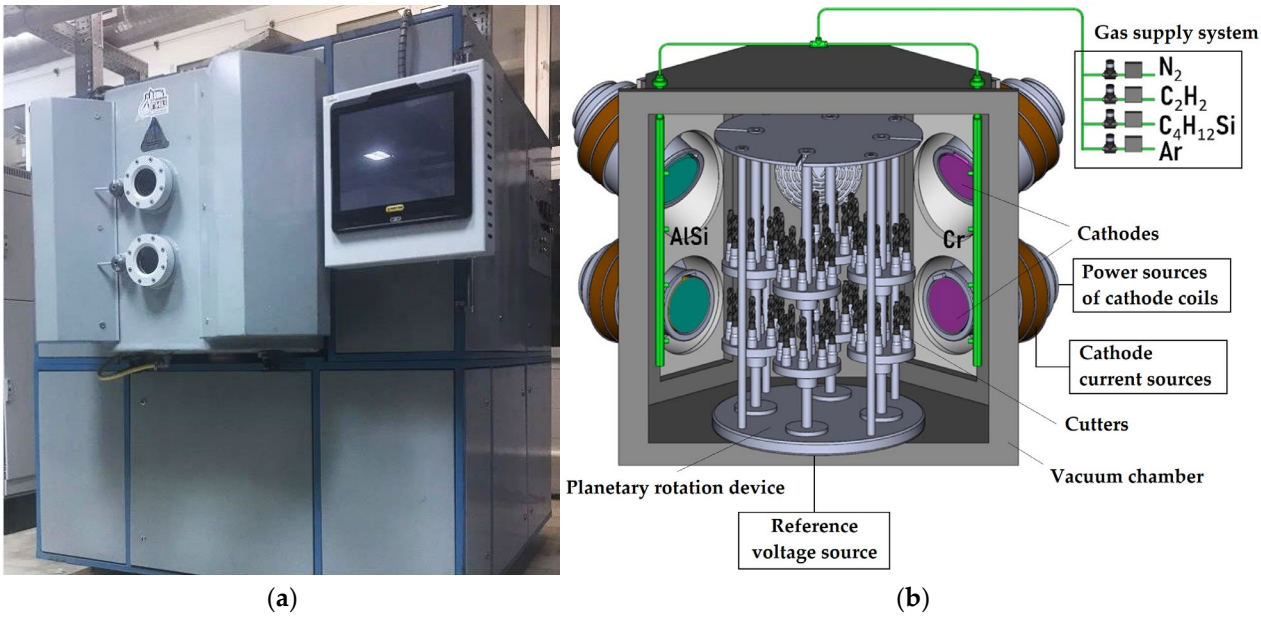

Figure 3. General view (**a**) and internal design of the processing unit (**b**) used for (CrAlSi)N/DLC-Si coatings deposition on SiAlON-ceramic samples.

2.3. Methods for Studying the Structure, Elemental Composition, and Tribological Testing of Samples of SiAlON Ceramics with (CrAlSi)N/DLC-Si Coatings

X-ray Photoelectron Spectroscopy (XPS) analysis was used to study carbon atoms' chemical and electronic state on the surface of ceramic samples with (CrAlSi)N/DLC-Si coatings. The DLC and (CrAlSi)N/DLC-Si coated samples and uncoated ones were heated to 800 °C in a high-temperature vacuum furnace Thermionic T1 (JSC Thermionika, Podolsk, Moscow region, Russia) and analyzed. Preheating was carried out to predict the transformation of the initial structure of the (CrAlSi)N/DLC-Si coatings during cutting, which is accompanied by the development of high temperatures.

XPS analysis was performed on a Thermo Scientific K-ALPHA X-ray photoelectron spectrometer (Thermo Fisher Scientific Inc., Bremen, Germany). High-resolution imaging was carried out using monochromatic and polychromatic Mg Kα and Al Kα radiation at a power of 200–300 W, a voltage of 14 kV, and a chamber pressure of 7×10^{-8} Pa. Studies were carried out to identify various peaks of the DLC layer in the composition of the prominent C1s peak: sp2 and sp3 peaks characterizing carbon hybridizations, and C=O and C-O peaks characterizing various compounds of components with oxygen and other elements. In addition, the peaks of phases containing silicon compounds were analyzed. A set of characteristics was evaluated during XPS analysis such as start binding energy (SBE), binding energy (BE), end binding energy (EBE), and atomic percent (Atomic %) for each component of the DLC layer.

The study of the elemental composition of the surface layer of ceramic samples with (CrAlSi)N/DLC-Si coatings was carried out using the Oxford Instruments INCA Energy energy-dispersive X-ray spectroscopy (EDX) system with which a VEGA 3 LMH scanning electron microscope (Tescan, Brno, Czech Republic) is equipped. The atoms were excited using a beam of electrons in the EDX process and emitted x-rays specific to each chemical element. When studying the energy spectrum of this radiation using a specialized program, data were obtained on the samples' semi-quantitative elemental composition.

The study of the structure of the formed coatings was carried out by transmission electron microscopy using JEM-2100F equipment (JEOL, Tokyo, Japan). The surface microrelief of ceramic samples with (CrAlSi)N/DLC-Si coatings was studied on a DektakXT stylus profilometer (Bruker, Karlsruhe, Germany).

The nanohardness of (CrAlSi)N/DLC-Si coatings formed on Si-AlON-ceramic samples was estimated on the Martens scale by indentation with a diamond indenter on a CSEM instruments' nanohardness tester (CSM Instruments SA, Peseux, Switzerland) according to the method of Oliver and Farr, [50–53]. The cycle "load–unload" duration was 50 s, and the applied load was 4.0 mN. The nanohardness and modulus of elasticity of the coatings were calculated based on the obtained experimental data.

Wear resistance of coated ceramic specimens under conditions of high-temperature friction-sliding in contact with a counterbody (ceramic ball of 6 mm in diameter) at a load of 1 N, a sliding speed of 10 cm/s, a displacement radius of 2 mm, and a heating temperature of 800 °C was evaluated on a TNT tribometer S-AX0000 (Anton Paar TriTec SA, Wien, Austria). The change in the coefficient of friction over time was determined with the rotation of the test sample relative to a fixed counterbody. The reduced volumetric wear of the coated samples was determined using the average value of the cross-sectional area of the wear track, which was estimated from the results of measuring five transverse profiles of the wear track on the DektakXT profilometer.

2.4. Wear Test Technique for End Mills of SiAlON Ceramics with (CrAlSi)N/DLC-Si Coatings

Laboratory testing of uncoated and (CrAlSi)N/DLC-Si coated SiAlON-ceramic end mills was carried out by high-speed cutting of aviation nickel-chromium alloy – NiCr20TiAl (EN 10269), which had the shape of a cylinder with a diameter of 50 mm. The chemical composition of the NiCr20TiAl alloy is shown in Table 1. Physical and mechanical properties of the nickel-chromium alloy to be machined are as follows: HRC hardness of 32–33; ultimate strength (tensile strength) of 1130–1160 MPa; density of 5.66 g/cm^3.

Table 1. Chemical composition (%) of NiCr20TiAl nickel-chromium alloy.

Ni	Cr	Ti	Al	Fe	Si	Co	Mn	Cu	C	Other Elements
73	20	2.5	1.0	1.0	0.6	0.5	0.4	0.2	0.07	0.73

The tests were carried out on a CTX 1250TC multi-axis turning and milling machining center from DMG (Bielefeld, Germany). The positioning of SiAlON-ceramic end mills relative to the workpiece made of NiCr20TiAl alloy during wear resistance tests is shown in Figure 4a. The experiments were carried out under the following milling modes: cutting speed of 376.8 m/min (rotational speed 12,000 rpm), feed per minute of 1500 mm/min, and feed per tooth of 0.03 mm/tooth. The "dry" machining scheme without cutting fluids was used [54].

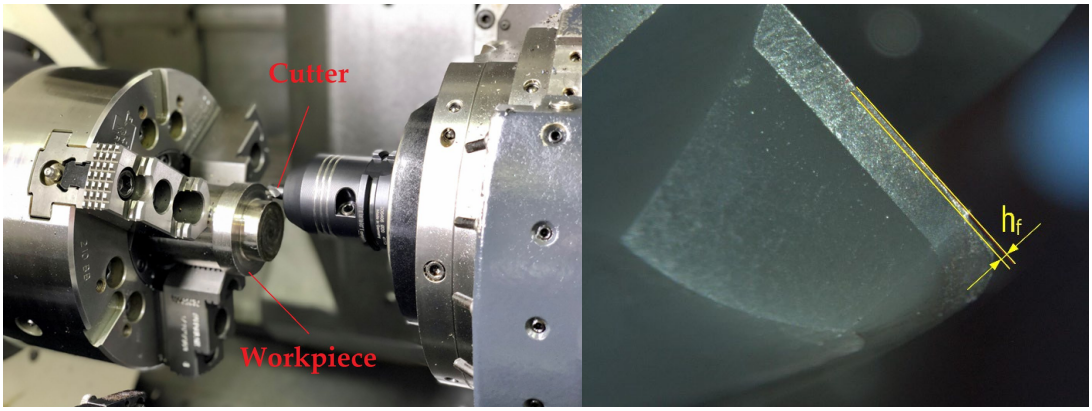

(**a**) (**b**)

Figure 4. Positioning of end mills made of SiAlON ceramics relative to the workpiece made of NiCr20TiAl alloy for wear resistance testing (**a**) and the wear center location on the back surface of the cutting tooth and measuring h_f in quantifying wear (**b**).

The critical size of the wear area h_f along the flank surface of the cutter tooth equal to 0.4 mm was taken as the criterion of the end mills' failure (Figure 4b). The wear resistance of the tool was defined as the cutting time until the cutter reaches the specified wear. When the mentioned criterion is exceeded, the cases of chipping of the cutting edge increase many times over. A SteREO Discovery V12 metallographic optical microscope from Zeiss (Oberkochen, Germany) was used to quantify wear. The wear pad was monitored on each of the tested ceramic cutter teeth. The arithmetic mean values were calculated based on the obtained data, which were used to draw the "wear-cutting time" curves.

3. Results and Discussion

3.1. Structure and Morphology of (CrAlSi)N/DLC-Si Coatings Deposited on SiAlON Ceramics

The results of studies performed by means of transmission electron microscopy of the cross-section of (CrAlSi)N/DLC-Si coatings deposited on SiAlON ceramics make it possible to reveal the structural features of the DLC-Si outer layer (Figure 5). The DLC-Si layer formed by chemical vapor deposition in a mixture of acetylene, argon, and tetramethylsilane is characterized by a homogeneous amorphous structure, on which the gradient DLC layer and the main DLC layer are well pronounced. It should be noted that no microstructural differences were observed in the coatings formed at different contents of tetramethylsilane $Si(CH_3)_4$.

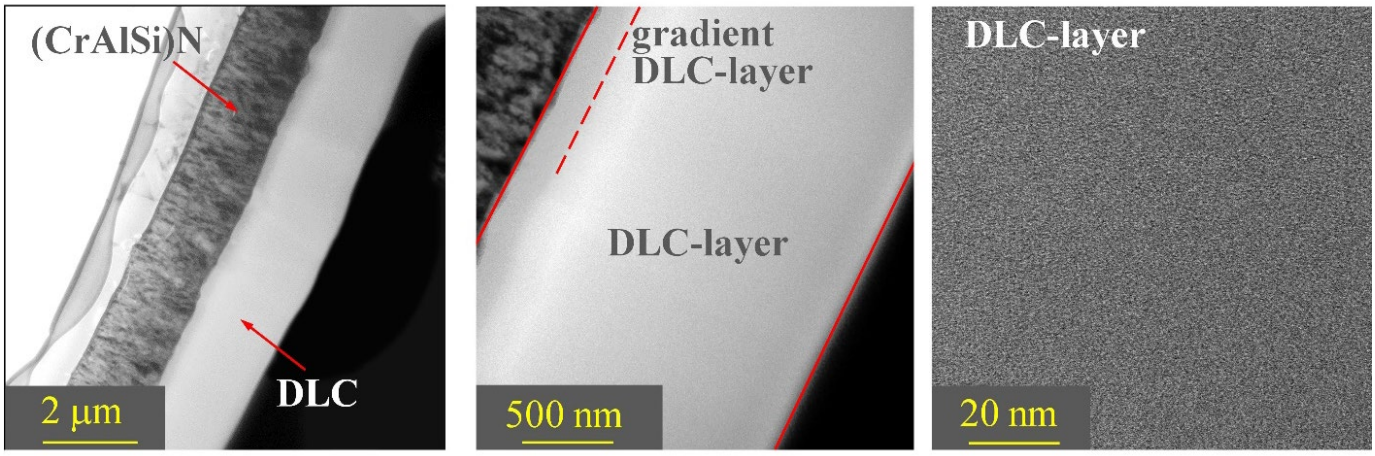

Figure 5. TEM images of the cross-section of the (CrAlSi)N/DLC-Si coating (**a**,**b**) and the DLC-Si outer layer (**c**).

The distinctive features of the (CrAlSi)N/DLC-Si coatings are revealed by SEM analysis and 3D surface profilometry (Figure 6). The surface of (CrAlSi)N/DLC-Si coatings has a characteristic morphology of densely packed rounded granule-like particles with a diameter of 300–900 nm. A similar morphological pattern was observed by the authors of [55] in studying DLC coatings.

3.2. Structure and Elemental Composition of the Surface Layer of (CrAlSi)N/DLC-Si Coatings Deposited on SiAlON Ceramics

Tables 2–5 summarize the results of the XPS analysis of (CrAlSi)N/DLC-Si coatings formed on SiAlON-ceramic at various contents of 1, 4, 7, and 10% vol. of tetramethylsilane $Si(CH_3)_4$ in a gas mixture with acetylene and argon. Considering that an excess amount of oxygen on the surface of the samples complicates the assessment of sp2 and sp3 hybridizations of carbon, a thin surface layer of the coating was etched with argon ions with an energy of 2 keV to a depth of about 0.005 μm immediately before analysis. The error in determining the binding energy of electronic levels in the XPS analysis was 0.1 eV.

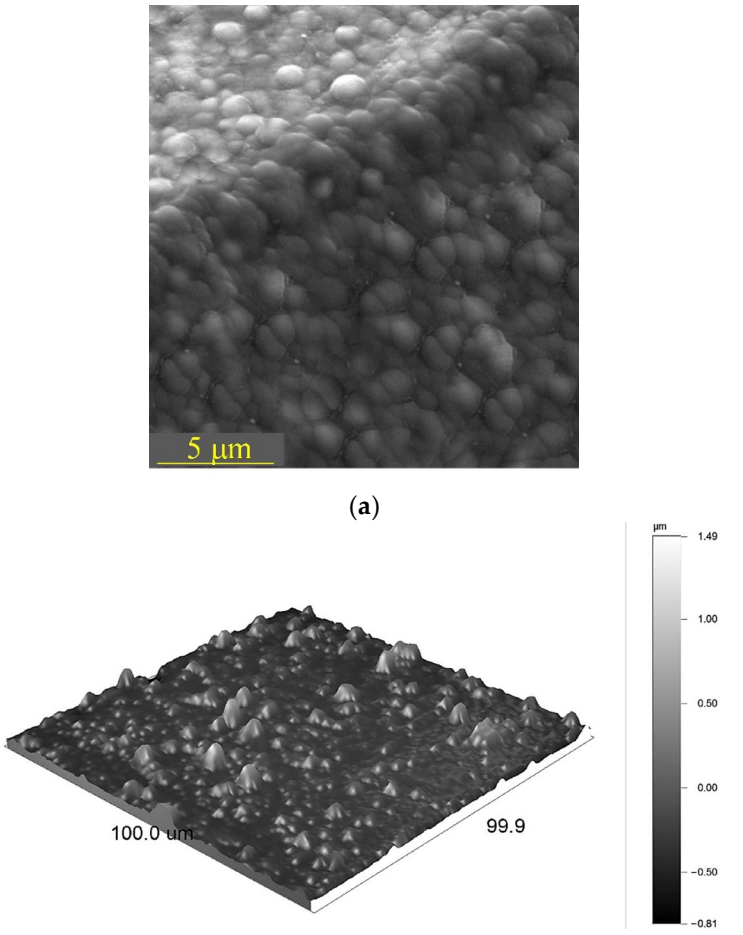

Figure 6. SEM image of the surface of the (CrAlSi)N/DLC-Si coating formed on the cutting edge of the end mill (**a**) and its 3D profilogram (**b**).

Table 2. XPS spectra and peak energy characteristics of (CrAlSi)N/DLC-Si coatings (DLC-Si layer deposition in 1% vol. $Si(CH_3)_4$, 54% vol. Ar, and 45% vol. C_2H_2).

XPS-Peak	Scanning Range, eV	Binding Energy Peak, eV	Atomic % (Initial Sample)	Atomic % (after Heating)
C1s Sp3 (hybridization of diamond)	279–297	285.5	56.34	33.67
C1s Sp2 (hybridization of graphite)	279–297	284.3	18.31	28.08
C1s C=O	279–297	286.5	9.31	13.12
C1s C-O	279–297	286.2	7.46	10.97
O1s C-O	525–545	533.4	3.89	7.03
O1s C=O	525–545	531.8	3.59	6.01
O1s SiO_2	525–545	532.5	N/D	1.12
Si2p3, Si-N, Si-C	95–110	100.4	1.1	-

Table 3. XPS spectra and peak energy characteristics of (CrAlSi)N/DLC-Si coatings (DLC-Si layer deposition in 4% vol. $Si(CH_3)_4$, 51% vol. Ar, and 45% vol. C_2H_2).

XPS-Peak	Scanning Range, eV	Binding Energy Peak, eV	Atomic % (Initial Sample)	Atomic % (after Heating)
C1s Sp3 (hybridization of diamond)	279–297	285.3	56.02	39.49
C1s Sp2 (hybridization of graphite)	279–297	284.5	15.53	21.98
C1s C=O	279–297	286.5	9.41	11.89
C1s C-O	279–297	286.1	7.73	9.41
O1s C-O	525–545	533.5	3.68	6.86
O1s C=O	525–545	531.8	3.35	6.02
O1s SiO_2	525–545	532.4	N/D	3.35
Si2p3, Si-N, Si-C	95–110	100.3	4.28	1.0

Table 4. XPS spectra and peak energy characteristics of (CrAlSi)N/DLC-Si coatings (DLC-Si layer deposition in 7% vol. $Si(CH_3)_4$, 48% vol. Ar, and 45% vol. C_2H_2).

XPS-Peak	Scanning Range, eV	Binding Energy Peak, eV	Atomic % (Initial Sample)	Atomic % (after Heating)
C1s Sp3 (hybridization of diamond)	279–297	285.2	51.94	31.23
C1s Sp2 (hybridization of graphite)	279–297	284.5	15.48	25.02
C1s C=O	279–297	286.5	10.02	12.74
C1s C-O	279–297	286.2	8.03	10.31
O1s C-O	525–545	533.4	4.77	7.94
O1s C=O	525–545	531.6	3.34	6.01
O1s SiO_2	525–545	532.4	1.01	5.71
Si2p3, Si-N, Si-C	95–110	100.4	5.41	1.04

Table 5. XPS spectra and peak energy characteristics of (CrAlSi)N/DLC-Si coatings (DLC-Si layer deposition in 10% vol. $Si(CH_3)_4$, 45% vol. Ar, and 45% vol. C_2H_2).

XPS-Peak	Scanning Range, eV	Binding Energy Peak, eV	Atomic % (Initial Sample)	Atomic % (after Heating)
C1s Sp3 (hybridization of diamond)	279–297	285.3	48.1	31.02
C1s Sp2 (hybridization of graphite)	279–297	284.3	15.21	23.1
C1s C=O	279–297	286.6	11.39	12.98
C1s C-O	279–297	286.1	8.17	10.02
O1s C-O	525–545	533.5	5.39	8.1
O1s C=O	525–545	531.8	3.63	6.72
O1s SiO_2	525–545	532.5	1.05	6.01
Si2p3, Si-N, Si-C	95–110	100.5	7.06	2.05

It can be seen that the C1s carbon peak was the main component of the coatings' surface under study. Its scanning was carried out in the energy range from 279 to 297 eV, and the spectrum acquisition time was 80 min. Two main states can be distinguished in the carbon spectrum, sp3 and sp2 hybridization of carbon, which are related to diamond and graphite, respectively, and have binding energies of about 284.3–285.5 eV. The share of sp3/sp2 hybridizations accounts for about 63–74% of the total components' composition of the studied coatings in the initial state. In addition, XPS analysis revealed various carbon-containing impurities (about 16–19%) in the main peak of the C1s coating, which is typical for DLC films [56–58]. In the analysis of samples with coatings in the initial state (without heating and exposure), sp3 carbon hybridization significantly predominates over sp2 (by 3.1–3.3 times) for all samples under study.

The XPS analysis also revealed an O1s peak during scanning in the energy range from 525 to 545 eV, which characterizes the presence of various forms of oxygen with increased binding energies, 531.6–533.5 eV. The studied samples contain oxygen in the form of surface-adsorbed groups. The proportion of the oxygen component for the samples in the initial state is about 7–10%. It should be noted that another component in the main oxygen peak O1s was identified as silicon dioxide SiO_2 for samples on which the DLC-Si layer was deposited in a gas mixture containing 7 and 10% vol. of $Si(CH_3)_4$. Its share was about 1%.

In addition, a Si2p3 silicon photoelectron peak was detected, indicating the presence of Si, Si-N, Si-C type compounds with energies connections of 100.3–100.5 when scanning (CrAlSi)N/DLC-Si coatings in the energy range from 95 to 110 eV in the XPS analysis. For the samples at the initial state, its proportion increased from 1.1 to 7.06% as $Si(CH_3)_4$ increased from 1 to 10% vol. in the gas mixture during the DLC-Si layer deposition.

The last column of Tables 2–5 shows the calculated data of the XPS analysis of the samples after heating in a vacuum furnace to a temperature of 800 °C and holding for 30 min. The data obtained indicate a significant transformation in the DLC-Si layer structure upon thermal treatment. An analysis of these changes is of particular interest since the surface layer of tools made of SiAlON ceramics is subjected to intense thermal impact during operation at high cutting speeds. The main changes identified are as follows:

- Firstly, pronounced changes in the C1s carbon peak were established as follows: The share of sp3/sp2 hybridization among the total composition of the components of the coatings under study decreases by 9–13%. Simultaneously, the proportion of diamond hybridization (sp3) significantly decreases by 17–23%, while the proportion of graphite hybridization (sp2) increases by 6–10%. The proportion of various carbon-containing impurities in the DLC-Si layer increases by 4–7%. The specified tendency for the transition of sp3- to sp2-hybridization under thermal exposure is due to the level of thermal stability and features of the interatomic bonds of carbon atoms and is consistent with the experimental data of other researchers [59–62].
- Secondly, significant changes in the O1s oxygen peak were revealed. Its fraction in the composition of the DLC-Si layer's components for samples subjected to high-temperature treatment increases by about 2 times compared to the initial samples. At the same time, the proportion of silicon dioxide SiO_2 in the oxygen peak O1s for the samples after thermal treatment increases significantly as $Si(CH_3)_4$ increases in the gas mixture during the DLC-Si layer deposition. If $Si(CH_3)_4$ content is 1% vol., the proportion of SiO_2 is about 1%. Then, the share of silicon dioxide in the DLC-Si layer's composition is 3.3, 5.6, and 6% at 4, 7, and 10% vol. of $Si(CH_3)_4$, respectively. Simultaneously, there is a significant decrease in the proportion of the Si2p3 silicon peak (compounds of the Si, Si-N, Si-C type) in the surface layer of the samples after heating. It indicates the oxidative reactions' occurrence with the thermostable SiO_2 phases' formation that reduces the compressive stress in the films and improves the film fracture toughness [63]. The authors of [64] reported an increase in the wear resistance of DLC:Si films two times in comparison with pure DLC films. The authors of [65] noted that analysis of the XPS peaks of DLC:Si films containing 4–29 at.% of Si deposited by reactive magnetron sputtering revealed the presence of Si–C bonds and a significant amount of Si–O–C and Si–O_x bonds. However, the rest of the mentioned study [65] is devoted to researching the optical properties of those coatings. The intensification of the formation of these phases occurs, starting from temperatures of 800 °C as follows from the data of works [66,67].

Since the performed XPS analysis provides information on the presence of various compounds in a thin near-surface layer and does not provide information on the elemental composition and content of the alloying element (silicon) along the depth of the surface layer, the EDX analysis of the samples was additionally performed. The EDX maps of the distribution of chemical elements in a tool SiAlON-ceramic sample coated with (CrAlSi)N/DLC-Si (as an example, a characteristic pattern for the deposition of a DLC-Si

layer at 4% vol. in a gas mixture) is presented in Figure 7. It allows us to qualitatively assess the various elements' concentration in the surface layer from contrast images. In particular, the content of silicon is traced in the bulk of the SiAlON-ceramic, in the preliminarily formed nitride layer (CrAlSi)N, and directly on the surface of the formed DLC-Si layer.

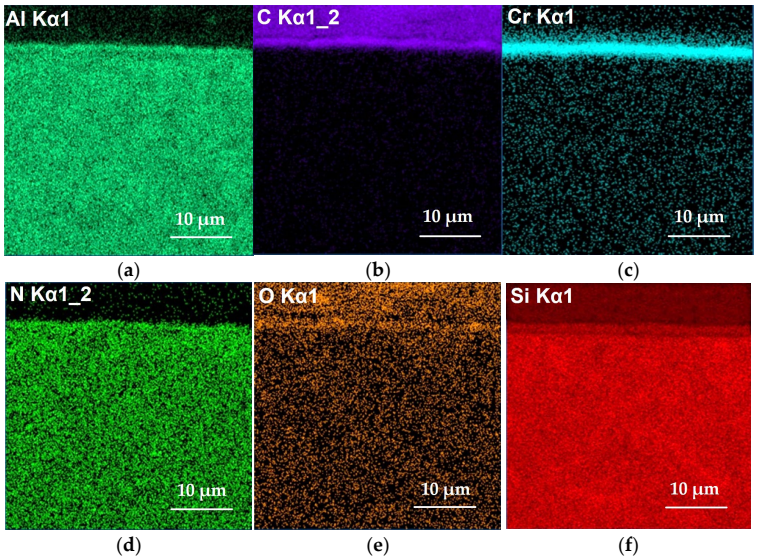

Figure 7. EDX-maps of the chemical elements' distribution in the surface layer of a sample made of SiAlON ceramics with (CrAlSi)N/DLC-Si coatings: (**a**) aluminum; (**b**) carbon; (**c**) chromium; (**d**) nitrogen; (**e**) oxygen; (**f**) silicon.

Figure 8 shows the distribution of elements over the cross-section of a (CrAlSi)N/DLC-Si coating formed on a sample of SiAlON tool ceramics. It is seen that the silicon concentration increases upon transition from the main DLC layer to the gradient DLC layer (the layer structure is visible in Figure 5b), then it slightly decreases along the depth of the intermediate (CrAlSi)N layer and sharply increases along the depth of the SiAlON ceramics.

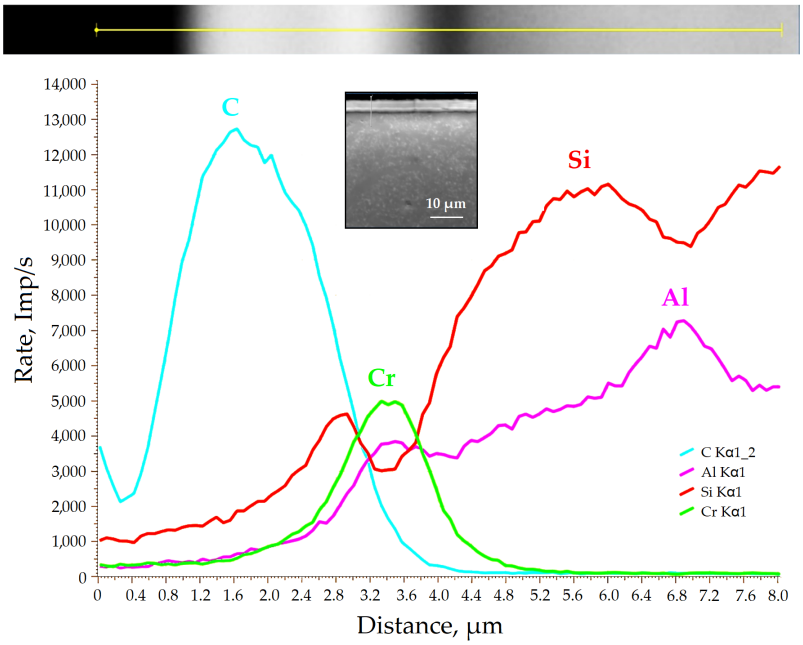

Figure 8. Elements' distribution over the cross-section of the (CrAlSi)N/DLC-Si coating deposited on a sample of tool SiAlON-ceramic. (Data obtained by EDX analysis.)

Figure 9 shows the relationship between the content of tetramethylsilane in the gas mixture used during the primary (outer) DLC-Si layer deposition and the silicon content in it, revealed by the results of XPS analysis. It can be seen that the dependence is linear, and the content of the mass fraction of Si (% wt.) increases monotonically with an increase in the $Si(CH_3)_4$ content in the gas mixture (% vol.). Thus, the presence of 1, 4, 7, and 10% vol. $Si(CH_3)_4$ in the gas mixture ensures the Si content in the DLC-Si layer is about 1.5, 4.1, 6.2, and 7.7% wt.

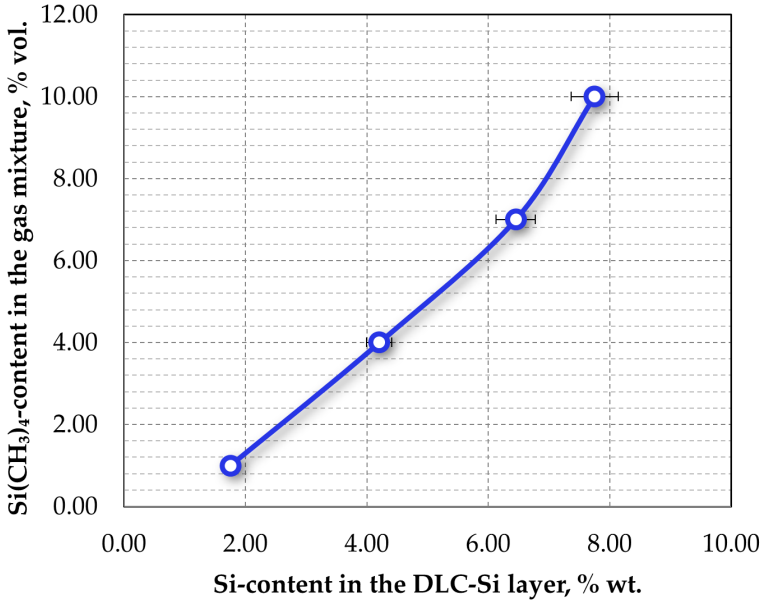

Figure 9. Dependence of the Si mass content in the main DLC-Si layer on the volume content of $Si(CH_3)_4$ in the gas mixture. (Data obtained by EDX analysis.)

3.3. Physical, Mechanical, and Tribological Characteristics of the Surface Layer of (CrAlSi)N/DLC-Si Coatings Deposited on SiAlON Ceramics

The dominant role in forming DLC coatings' various properties such as hardness and elastic modulus coefficient of friction, and volumetric wear, is played by the structural configurations of carbon and alloying/doping elements' compounds present in the deposited coating. Table 6 shows the results of the assessment of nanohardness and modulus of elasticity for polished samples of SiAlON ceramics with (CrAlSi)N/DLC-Si coatings with different Si content in the outer DLC layer, provided by varying the content of $Si(CH_3)_4$ in a gas mixture after deposition. The results were obtained at a penetration depth of the Berkovich indenter of about 400 nm. It can be seen that as the proportion of carbon sp3 bonds decreases and the proportion of silicon compounds increases, the nanohardness (H) and elastic modulus (E) of the DLC-Si layer decrease compared to the "pure" DLC film deposited in the absence of a silicon-containing gas. For example, while the values of H and E for the DLC layer are 28 and 246 GPa, these values decrease to 19 and 198 GPa, respectively, for the DLC-Si layer at Si, 7.7% wt.

Table 6. Characteristics of (CrAlSi)N/DLC-Si coatings deposited on SiAlON-ceramic substrates with different Si contents in the outer layer.

Sample	Si-Content in DLC Layer, % wt.	Nanohardness H, GPa	Modulus of Elasticity E, GPa
Original	-	28 ± 1.5	246 ± 6
No. 1	1.5	27 ± 1	241 ± 8
No. 2	4.1	26 ± 1.5	238 ± 6
No. 3	6.2	22 ± 1	210 ± 6
No. 4	7.7	19 ± 1	198 ± 4

It should be noted that the obtained nanohardness (H) and elastic modulus (E) of the DLC-Si layer correlates with the data obtained in [63] for hardness and elastic modulus of DLC films doped with Si deposited on the glass substrate and even surpass them even for the classic DLC-coating: 24 ± 2 and 159 ± 4 GPa, correspondingly.

However, it is impossible to predict the behavior of (CrAlSi)N/DLC-Si coatings under the simultaneous action of thermal and mechanical loads typical for the operation of a cutting tool only based on the established values of nanohardness and elastic modulus. Thus, the evaluating results of the effect of the Si content in the DLC-Si layer on the coefficient of friction and volumetric wear of the surface layer of SiAlON samples under high-temperature exposure are of interest.

Figure 10 shows the results of tribological tests for samples made of SiAlON ceramics with (CrAlSi)N/DLC-Si coatings with different Si-content (1.5, 4.1, 6.2, and 7.7% wt.). Additional data obtained for uncoated samples made of SiAlON ceramics and samples with single-layer coatings such as (CrAlSi)N and "pure" DLC are shown in Figure 11 for comparison.

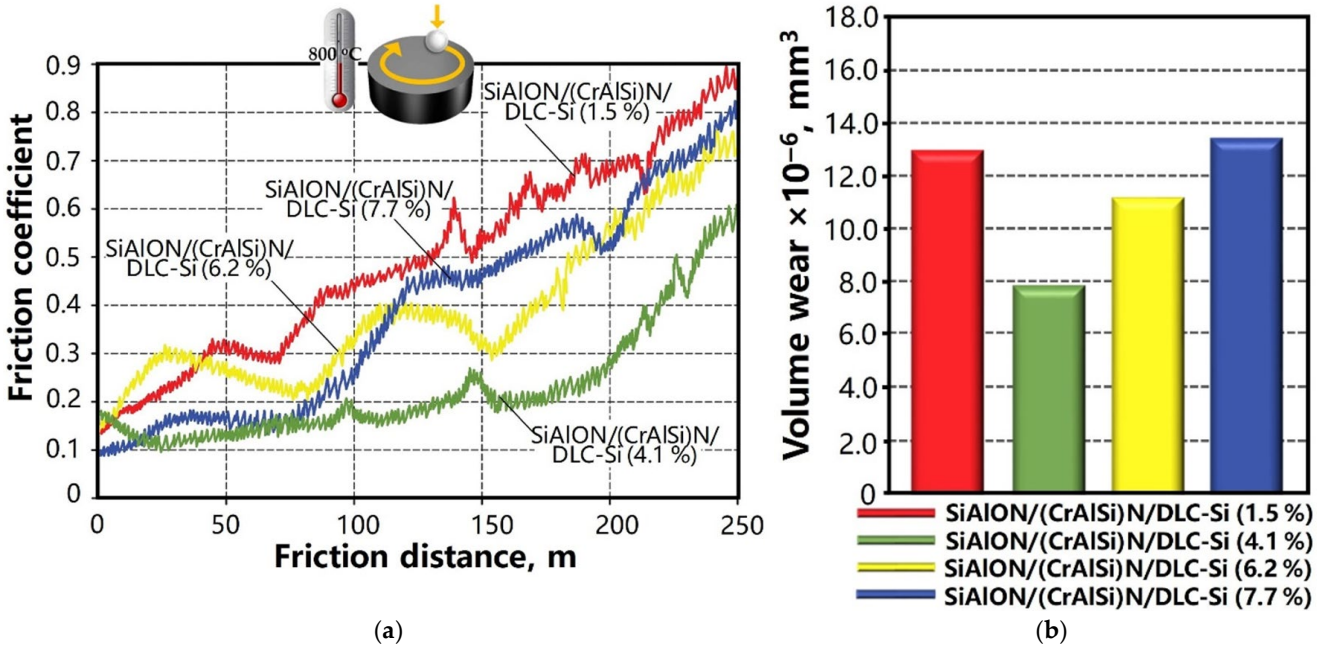

(**a**) (**b**)

Figure 10. Change in the coefficient of friction depending on the testing time of samples made of SiAlON ceramics with (CrAlSi)N/DLC-Si coatings (**a**) and volumetric wear of samples after passing a distance of 250 m at high-temperature friction-sliding (**b**).

The presented results allow us to conclude (Figure 10) that the deposited (CrAlSi)N/DLC-Si coatings with different silicon content reduce the coefficient of friction of SiAlON ceramics over a 150 m test distance. After that, it increases significantly for samples with a Si content of 1.5, 6.2, and 7.7% wt. Upon reaching 250 m, it already has values characteristic of the original SiAlON ceramics and "pure" DLC coatings (Figure 11). The coefficient of friction of silicon-free DLC coatings begins to increase sharply already after passing a distance of 50 m and quickly reaches values corresponding to the ceramic substrate. It can be explained by the well-known low thermal stability of "pure" DLC coatings. Volumetric wear of the (CrAlSi)N/DLC-Si coated samples with the Si content of 1.5 and 7.7% wt was slightly less than for those made of SiAlON ceramics. Only a sample with a silicon content of about 4.1% wt had a lower coefficient of friction throughout the entire friction distance than SiAlON ceramics and "pure" DLC coatings. The same coating was distinguished by the most negligible volumetric wear, determined in the cross-section of the worn friction path. The authors of [63] also noted the primary influence of the content of SiO_x (O/Si ratio in DLC:SiO_x films was 0.286 ± 0.008) on the wear resistance of coatings for sliding/friction parts such as bearings or for precision gages.

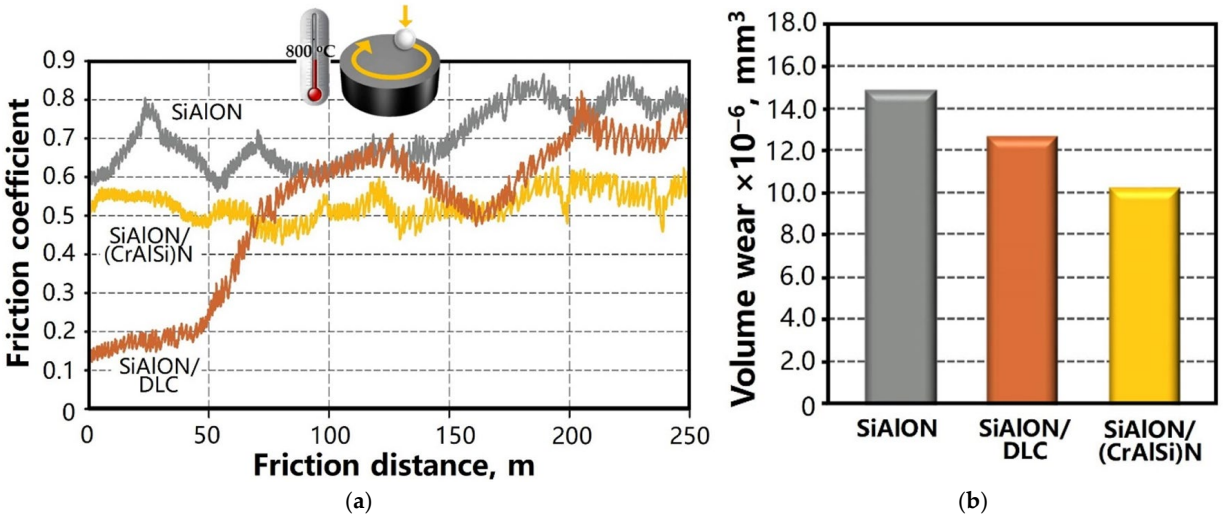

Figure 11. Change in the coefficient of friction depending on the testing time of uncoated samples made of SiAlON ceramics and with the deposited single-layer (CrAlSi)N and DLC coatings (**a**) and volumetric wear of samples after passing a distance of 250 m at high-temperature friction-sliding (**b**).

The results obtained are related to the fact that samples with (CrAlSi)N/DLC-Si coatings with a silicon content of about 4.1% wt. have the most minor decrease in the proportion of diamond sp3 hybridization in the structure upon heating (Table 3), and doping silicon in carbon coating makes it possible to increase its thermal stability due to the formation of SiO_2 compounds under thermal action, which was identified by the XPS analysis described above. It can be assumed that for a sample with a lower silicon content of 1.5% wt., the amount of SiO_2 formed during heating is still insufficient for a noticeable increase in the thermal stability of the surface layer (Table 2). The insufficient effect of the use of (CrAlSi)N/DLC-Si coatings with a higher silicon content (6.2 and 7.7% wt.) can be attributed to the fact that despite an increase in the amount of SiO_2 formed during thermal exposure (Tables 4 and 5), this compound possessing thermal stability exhibits also increased brittleness reported by various authors [68,69]. Knowing the wear-resistant properties of SiO_x content in DLC coatings, the authors [70] even propose the deposition of SiO_2 quartz film as an independent layer on Al_2O_3 ceramics in combination with DLC coating on top of it. Perhaps that is why the rather intensive wear is observed under the mechanical action of the counterbody on the surface layer of these samples. In addition, the lowest values of H and E were recorded for these samples (Table 6), which will significantly decrease during the thermal action on the surface layer.

When analyzing the behavior of (CrAlSi)N/DLC-Si coatings during high-temperature friction-sliding, the possible role of the intermediate (CrAlSi)N nitride coating, which in itself reduces the friction coefficient and the volumetric wear of the surface layer in the friction track, should be noted (Figure 11). Multi-component coatings of this type have proven well during operation under conditions of temperature influence, and their high thermal stability among nitride coatings was reported in [71,72]. It can be assumed that the outer DLC-Si layer of the two-layer (CrAlSi)N/DLC-Si coating composition performs antifriction functions and protects the surface layer from intense wear at the initial stage. After it loses its wear-resistant properties, the intermediate layer (CrAlSi)N perceives effective thermal and mechanical loads, providing less intensive volumetric wear of SiAlON ceramics.

It was shown that the (CrAlSi)N/DLC-Si coating with a Si content of about 4.1% wt exhibits the best wear resistance considering the results of tribological tests. This coating deposited on SiAlON-ceramic end mills has been selected for laboratory testing in milling of NiCr20TiAl nickel-chromium alloy.

3.4. Wear Resistance of SiAlON-Ceramic End Mills with (CrAlSi)N/DLC-Si Coatings

Two groups of SiAlON-ceramic end mills (each group included four cutters) were subjected to wear resistance tests during cutting: the samples without coatings and with (CrAlSi)N/DLC-Si coatings (Si of ~4.1% wt.). Figure 12 shows cutting tool flank wear versus cutting time in milling of NiCr20TiAl alloy at a cutting speed of 376.8 m/min, a feed per minute of 1500 mm/min, and a feed per tooth of 0.03 mm/tooth. It can be seen that the deposition of (CrAlSi)N/DLC-Si coatings significantly (by 1.47) increases the wear resistance of cutters made of SiAlON ceramics (up to a failure criterion of 400 μm). Figure 13 shows optical images of the development of wear on the flank surface of the teeth of uncoated and coated (CrAlSi)N/DLC-Si end mills with an increase in cutting time, clearly demonstrating the decrease in the intensity of wear in the presence of the coating.

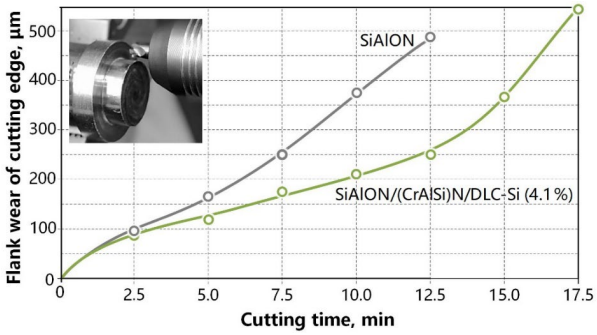

Figure 12. Dependences of flank wear of various SiAlON-ceramic end mills on cutting time in milling of NiCr20TiAl alloy.

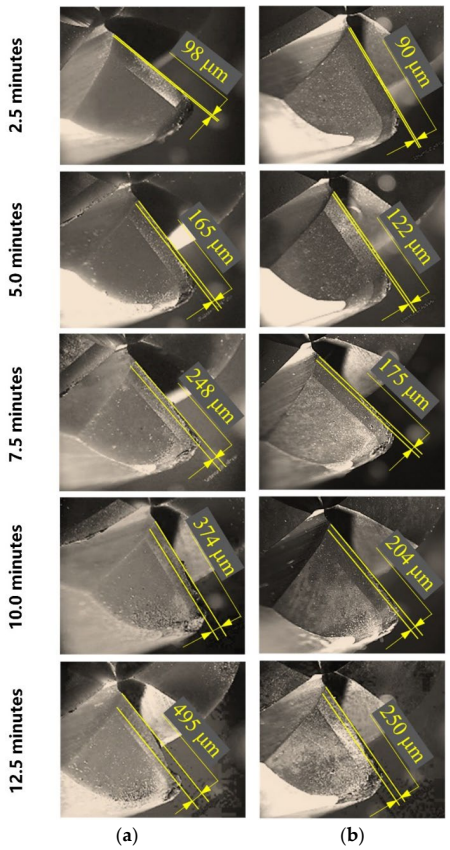

Figure 13. Optical images of the development of wear areas on the tooth flanks of uncoated (**a**) and (CrAlSi)N/DLC-Si-coated (**b**) SiAlON-ceramic end mills with an increase in cutting time.

Thus, the average operating time (wear resistance) of coated end mills before reaching the accepted failure criterion was 15.5 min and 10.5 min for the original cutters. Considering the extremely high cost of ceramic end mills, the achieved result of increasing wear resistance through the formation of (CrAlSi)N/DLC-Si coatings can provide a significant economic benefit.

It should be noted that a single-layer DLC coating is thermally unstable when heated at the mentioned temperature, as can be seen from high-temperature friction-sliding tests. However, the Si-doped DLC-coating combined with a three-component nitride sublayer demonstrated higher thermal stability. At the same time, the role of the substrate cannot be ignored. In this study, the substrate is a high-temperature-resistant material. It is obvious that if the studies were performed not for oxide-nitride ceramics but for less thermo-resistant material (for example, metal-based alloy), then the coating would demonstrate a different temperature tolerance.

4. Conclusions

This study has demonstrated that silicon doping of DLC coatings formed by gas-phase deposition in combination with the pre-formed interlayer coating deposition is an integrated approach that can expand the possible areas of application of diamond-like carbon coatings and increase the efficiency of their use for products operating under high thermal loads (primarily for cutting tools).

The EDX analysis showed that the presence of $Si(CH_3)_4$in the gas mixture in a volume of 1, 4, 7, and 10% ensures the formation of DLC coatings with a Si content of about 1.5, 4.1, 6.2, and 7.7% wt on SiAlON-ceramic samples, respectively.

XPS analysis showed that the main component of the structural state of the DLC-Si coatings formed by gas-phase deposition is diamond sp3 (share of 48–56%) and graphite sp2 (15–18%) hybridization of carbon. Under increased thermal exposure (heating up to 800 °C in a vacuum furnace), a significant transformation in the DLC-Si structure was revealed as follows: the fraction of sp3 significantly decreased (up to 23%), while the fractions of sp2 and carbon-containing impurities increased. In addition, a twofold increase in the fraction of the oxygen component in the DLC-Si coatings is noted upon heating. Simultaneously, oxidative reactions occur in the surface layer of the samples during heating with the formation of thermostable SiO_2 phases. Their fraction depends on the content of $Si(CH_3)_4$ in the gas mixture in the range of 1–6%.

Studies of the (CrAlSi)N/DLC-Si coatings' behavior in high-temperature friction-sliding have shown that the samples whose DLC coatings with ~4.1% wt. of silicon demonstrated the smallest coefficient of friction over the entire friction distance and the minimum volumetric wear of the surface layer at the friction path.

Tests of SiAlON-ceramic end mills in milling of NiCr20TiAl nickel-chromium alloy showed that the deposition of coatings of the rational (CrAlSi)N/DLC-Si composition (Si of ~4.1% wt.) made it possible to increase the operating time of the cutters by a factor of 1.47 compared to the uncoated ones.

The original experimental data can be used to develop DLC coatings for metalworking needs further.

Author Contributions: Conceptualization, M.A.V.; methodology, M.A.V.; software, M.A.V. and A.A.O.; validation, M.A.V.; formal analysis M.A.V.; investigation, M.A.V.; resources, M.A.V.; data curation, A.A.O.; writing—original draft preparation, M.A.V.; writing—review and editing, M.A.V.; visualization, M.A.V. and A.A.O.; supervision, M.A.V.; project administration, M.A.V.; funding acquisition, M.A.V. All authors have read and agreed to the published version of the manuscript.

Funding: This work was supported financially by the Ministry of Science and Higher Education of the Russian Federation (project No. FSFS-2023-0003).

Data Availability Statement: Data are available in a publicly accessible repository.

Acknowledgments: This study was carried out on the equipment of the Center of collective use of MSUT "STANKIN" supported by the Ministry of Higher Education of the Russian Federation (project No. 075-15-2021-695 from 26 July 2021, unique identifier RF 2296.61321 × 0013).

Conflicts of Interest: The authors declare no conflict of interest.

Appendix A

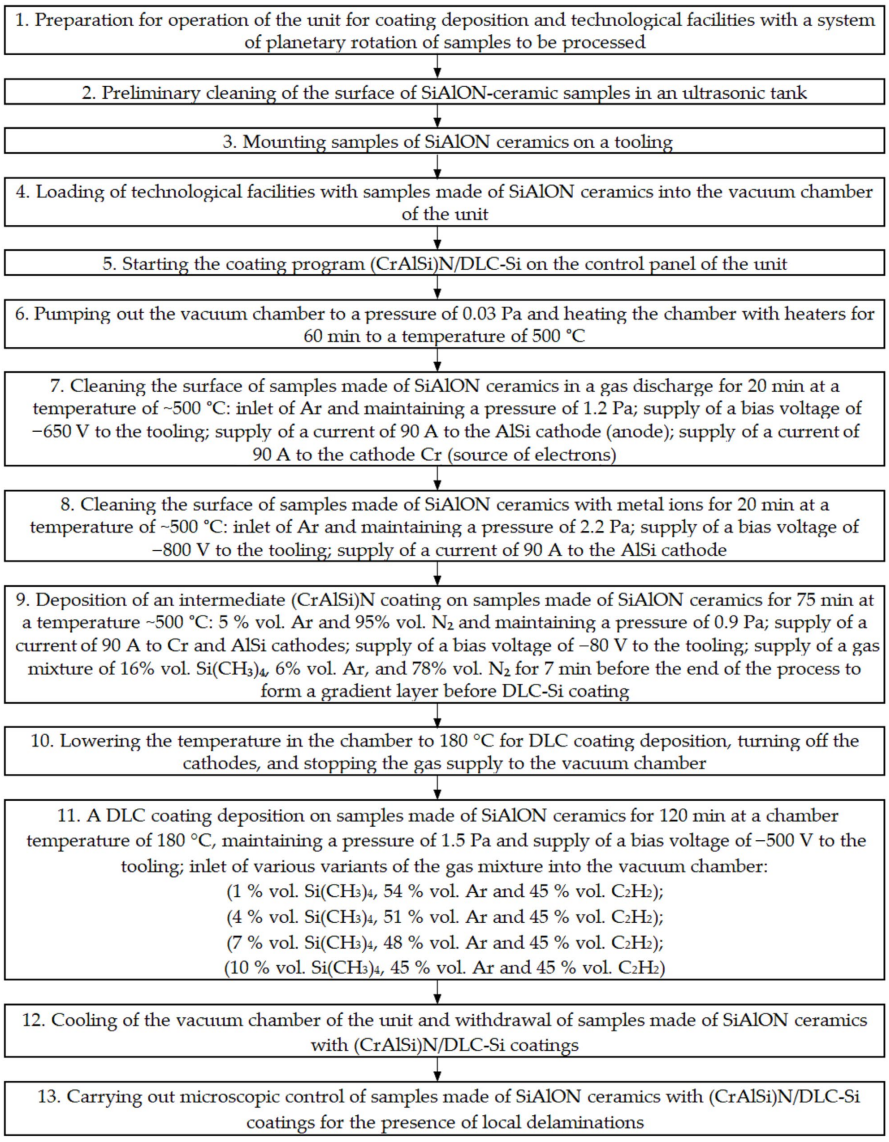

Figure A1. Flowchart of the technological process and the sequence of operations for (CrAlSi)N/DLC-Si coatings' deposition to samples made of SiAlON ceramics.

References

1. Tyagi, A.; Walia, R.S.; Murtaza, Q.; Pandey, S.M.; Tyagi, P.K.; Bajaj, B. A critical review of diamond like carbon coating for wear resistance applications. *Int. J. Refract. Met. Hard Mater.* **2019**, *78*, 107–122. [CrossRef]
2. Martins, P.S.; Magalhães, P.A.A.; Carneiro, J.R.G.; Talibouya Ba, E.C.; Vieira, V.F. Study of Diamond-Like Carbon coating application on carbide substrate for cutting tools used in the drilling process of an Al–Si alloy at high cutting speeds. *Wear* **2022**, *498–499*, 204326. [CrossRef]
3. Plotnikov, V.A.; Dem'yanov, B.F.; Yeliseeyev, A.P.; Makarov, S.V.; Zyryanova, A.I. Structural state of diamond-like amorphous carbon films, obtained by laser evaporation of carbon target. *Diam. Relat. Mater.* **2019**, *91*, 225–229. [CrossRef]
4. Fominski, V.Y.; Grigoriev, S.N.; Celis, J.P.; Romanov, R.I.; Oshurko, V.B. Structure and mechanical properties of W-Se-C/diamond-like carbon and W-Se/diamond-like carbon bi-layer coatings prepared by pulsed laser deposition. *Thin Solid Films* **2012**, *520*, 6476–6483. [CrossRef]

5. Rajak, D.K.; Kumar, A.; Behera, A.; Menezes, P.L. Diamond-Like Carbon (DLC) Coatings: Classification, Properties, and Applications. *Appl. Sci.* **2021**, *11*, 4445. [CrossRef]
6. Ohtake, N.; Hiratsuka, M.; Kanda, K.; Akasaka, H.; Tsujioka, M.; Hirakuri, K.; Hirata, A.; Ohana, T.; Inaba, H.; Kano, M.; et al. Properties and Classification of Diamond-Like Carbon Films. *Materials* **2021**, *14*, 315. [CrossRef]
7. Li, C.; Huang, L.; Yuan, J. Effect of sp^3 Content on Adhesion and Tribological Properties of Non-Hydrogenated DLC Films. *Materials* **2020**, *13*, 1911. [CrossRef]
8. Grigoriev, S.N.; Volosova, M.A.; Fedorov, S.V.; Mosyanov, M. Influence of DLC coatings deposited by PECVD technology on the wear resistance of carbide end mills and surface roughness of $AlCuMg_2$ and $41Cr_4$ workpieces. *Coatings* **2020**, *10*, 1038. [CrossRef]
9. Hatada, R.; Flege, S.; Ashraf, M.N.; Timmermann, A.; Schmid, C.; Ensinger, W. The Influence of Preparation Conditions on the Structural Properties and Hardness of Diamond-Like Carbon Films, Prepared by Plasma Source Ion Implantation. *Coatings* **2020**, *10*, 360. [CrossRef]
10. Gómez, I.; Claver, A.; Santiago, J.A.; Fernandez, I.; Palacio, J.F.; Diaz, C.; Mändl, S.; Garcia, J.A. Improved Adhesion of the DLC Coating Using HiPIMS with Positive Pulses and Plasma Immersion Pretreatment. *Coatings* **2021**, *11*, 1070. [CrossRef]
11. Liang, J.H.; Milne, Z.; Rouhani, M.; Lin, Y.-P.; Bernal, R.A.; Sato, T.; Carpick, R.W.; Jeng, Y.R. Stress-dependent adhesion and sliding-induced nanoscale wear of diamond-like carbon studied using in situ TEM nanoindentation. *Carbon* **2022**, *193*, 230–241. [CrossRef]
12. Wu, Y.; Li, H.; Ji, L.; Ye, Y.; Chen, J.; Zhou, H. Vacuum tribological properties of a-C:H film in relation to internal stress and applied load. *Tribol. Int.* **2014**, *71*, 82–87. [CrossRef]
13. Liu, X.; Yang, J.; Hao, J.; Zheng, J.; Gong, Q.; Liu, W. A near-frictionless and extremely elastic hydrogenated amorphous carbon film with self-assembled dual nanostructure. *Adv. Mater.* **2012**, *24*, 4614–4617. [CrossRef]
14. Zhang, T.; Pu, J.; Xia, Q.; Son, M.; Kim, K. Microstructure and nano-wear property of si-doped diamond-like carbon films deposited by a hybrid sputtering system. *Mater. Today Proc.* **2016**, *3*, S190–S196. [CrossRef]
15. Wang, L.; Nie, X.; Hu, X. Effect of Thermal Annealing on Tribological and Corrosion Properties of DLC Coatings. *J. Mater. Eng Perform* **2013**, *22*, 3093–3100. [CrossRef]
16. He, M.; Lee, S.; Yeo, C.-D. Investigating atomic structure of thin carbon film under mechanical stress and frictional heat generation. *Surf. Coat. Technol.* **2015**, *261*, 79–85. [CrossRef]
17. Meng, W.J.; Meletis, E.I.; Rehn, L.E.; Baldo, P.M. Inductively coupled plasma assisted deposition and mechanical properties of metal-free and Ti-containing hydrocarbon coatings. *J. Appl. Phys.* **2000**, *87*, 2840–2848. [CrossRef]
18. Zou, C.W.; Wang, H.J.; Feng, L.; Xue, S.W. Effects of Cr concentrations on the microstructure, hardness, and tempera-ture-dependent tribological properties of Cr-DLC coatings. *Appl. Surf. Sci.* **2013**, *286*, 137–141. [CrossRef]
19. Jeon, Y.; Park, Y.S.; Kim, H.J.; Hong, B.; Choi, W.S. Tribological properties of ultrathin DLC films with and without metal interlayers. *J. Korean Phys. Soc.* **2007**, *51*, 1124–1128. [CrossRef]
20. Bociaga, D.; Sobczyk-Guzenda, A.; Komorowski, P.; Balcerzak, J.; Jastrzebski, K.; Przybyszewska, K.; Kaczmarek, A. Surface Characteristics and Biological Evaluation of Si-DLC Coatings Fabricated Using Magnetron Sputtering Method on Ti6Al7Nb Substrate. *Nanomaterials* **2019**, *9*, 812. [CrossRef]
21. Wang, K.; Zhou, H.; Zhang, K.; Liu, X.; Feng, X.; Zhang, Y.; Chen, G.; Zheng, Y. Effects of Ti interlayer on adhesion property of DLC films: A first principle study. *Diam. Relat. Mater.* **2021**, *111*, 108188. [CrossRef]
22. Lubwama, M.; Corcoran, B.; McDonnell, K.; Dowling, D.; Kirabira, J.; Sebbit, A.; Sayers, K. Flexibility and frictional behaviour of DLC and Si-DLC films deposited on nitrile rubber. *Surf. Coat. Technol.* **2014**, *239*, 84–94. [CrossRef]
23. Almeida, E.A.; Milan, J.C.G.; da Costa, C.E.; Binder, C.; de Mello, J.D.B.; Costa, H.L. Combined Use of Surface Texturing, Plasma Nitriding and DLC Coating on Tool Steel. *Coatings* **2021**, *11*, 201. [CrossRef]
24. Aijaz, A.; Ferreira, F.; Oliveira, J.; Kubart, T. Mechanical properties of hydrogen free diamond-like carbon thin films deposited by high power impulse magnetron sputtering with Ne. *Coatings* **2018**, *8*, 385. [CrossRef]
25. Grigoriev, S.; Volosova, M.; Fyodorov, S.; Lyakhovetskiy, M.; Seleznev, A. DLC-coating Application to Improve the Durability of Ceramic Tools. *J. Mater. Eng. Perform.* **2019**, *28*, 4415–4426. [CrossRef]
26. Volosova, M.A.; Grigor'ev, S.N.; Kuzin, V.V. Effect of Titanium Nitride Coating on Stress Structural Inhomogeneity in Oxide-Carbide Ceramic. Part 4. Action of Heat Flow. *Refract. Ind. Ceram.* **2015**, *56*, 91–96. [CrossRef]
27. Gong, F.; Zhao, J.; Pang, J. Evolution of cutting forces and tool failure mechanisms in intermittent turning of hardened steel with ceramic tool. *Int. J. Adv. Manuf. Technol.* **2017**, *89*, 1603–1613. [CrossRef]
28. Bian, R.; Ding, W.; Liu, S.; He, N. Research on High Performance Milling of Engineering Ceramics from the Perspective of Cutting Variables Setting. *Materials* **2019**, *12*, 122. [CrossRef]
29. Vereschaka, A.A.; Grigoriev, S.N.; Volosova, M.A.; Batako, A.; Vereschaka, A.S.; Sitnikov, N.N.; Seleznev, A.E. Nano-scale multi-layered coatings for improved efficiency of ceramic cutting tools. *Int. J. Adv. Manuf. Technol.* **2017**, *90*, 27–43. [CrossRef]
30. Palmero, P. Structural Ceramic Nanocomposites: A Review of Properties and Powders' Synthesis Methods. *Nanomaterials* **2015**, *5*, 656–696. [CrossRef]
31. Vereschaka, A.S.; Grigoriev, S.N.; Sotova, E.S.; Vereschaka, A.A. Improving the efficiency of the cutting tools made of mixed ceramics by applying modifying nano-scale multilayered coatings. *Adv. Mat. Res.* **2013**, *712*, 391–394.
32. Bensouilah, H.; Aouici, H.; Meddour, I.; Yallese, M.A.; Mabrouki, T.; Girardin, F. Performance of coated and uncoated mixed ceramic tools in hard turning process. *Measurement* **2016**, *82*, 1–18. [CrossRef]

33. Volosova, M.; Grigoriev, S.; Metel, A.; Shein, A. The role of thin-film vacuum-plasma coatings and their influence on the efficiency of ceramic cutting inserts. *Coatings* **2018**, *8*, 287. [CrossRef]
34. Grigoriev, S.N.; Vereschaka, A.A.; Vereschaka, A.S.; Kutin, A.A. Cutting tools made of layered composite ceramics with nano-scale multilayered coatings. *Procedia CIRP* **2012**, *1*, 301–306. [CrossRef]
35. Grigoriev, S.N.; Volosova, M.A.; Fedorov, S.V.; Okunkova, A.A.; Pivkin, P.M.; Peretyagin, P.Y.; Ershov, A. Development of DLC-Coated Solid SiAlON/TiN Ceramic End Mills for Nickel Alloy Machining: Problems and Prospects. *Coatings* **2021**, *11*, 532. [CrossRef]
36. Sobol, O.V.; Andreev, A.A.; Grigoriev, S.N.; Gorban, V.F.; Volosova, M.A.; Aleshin, S.V.; Stolbovoi, V.A. Effect of high-voltage pulses on the structure and properties of titanium nitride vacuum-arc coatings. *Met. Sci. Heat Treat.* **2012**, *54*, 195–203. [CrossRef]
37. Lanigan, J.; Zhao, H.; Morina, A.; Neville, A. Tribochemistry of silicon and oxygen doped, hydrogenated diamond-like carbon in fully-formulated oil against low additive oil. *Tribol. Int.* **2015**, *82*, 431–442. [CrossRef]
38. Nakazawa, H.; Kamata, R.; Miura, S.; Okuno, S. Effects of frequency of pulsed substrate bias on structure and properties of silicon-doped diamond-like carbon films by plasma deposition. *Thin Solid Film.* **2015**, *574*, 93–98. [CrossRef]
39. Grigoriev, S.N.; Volosova, M.A.; Vereschaka, A.A.; Sitnikov, N.N.; Milovich, F.; Bublikov, J.I.; Fyodorov, S.V.; Seleznev, A.E. Properties of (Cr,Al,Si)N-(DLC-Si) composite coatings deposited on a cutting ceramic substrate. *Ceram. Int.* **2020**, *46*, 18241–18255. [CrossRef]
40. Uhlmann, E.; Hübert, C. Tool grinding of end mill cutting tools made from high performance ceramics and cemented carbides. *CIRP Ann.* **2011**, *60*, 359–362. [CrossRef]
41. Smirnov, K.L. Sintering of SiAlON ceramics under high-speed thermal treatment. *Powder Metall. Met. Ceram.* **2012**, *51*, 76–82. [CrossRef]
42. Chi, I.S.; Bux, S.K.; Bridgewater, M.M.; Star, K.E.; Firdosy, S.; Ravi, V.; Fleurial, J.-P. Mechanically robust SiAlON ceramics with engineered porosity via two-step sintering for applications in extreme environments. *MRS Adv.* **2016**, *1*, 1169–1175. [CrossRef]
43. Zheng, G.; Zhao, J.; Zhou, Y.; Li, A.; Cui, X.; Tian, X. Performance of graded nano-composite ceramic tools in ultra-high-speed milling of Inconel 718. *Int. J. Adv. Manuf. Technol.* **2013**, *67*, 2799–2810. [CrossRef]
44. Molaiekiya, F.; Stolf, P.; Paiva, J.M.; Bose, B.; Goldsmith, J.; Gey, C.; Engin, S.; Fox-Rabinovich, G.; Veldhuis, S.C. Influence of process parameters on the cutting performance of SiAlON ceramic tools during high-speed dry face milling of hardened Inconel 718. *Int. J. Adv. Manuf. Technol.* **2019**, *105*, 1083–1098. [CrossRef]
45. Metel, A.; Bolbukov, V.; Volosova, M.; Grigoriev, S.; Melnik, Y. Equipment for deposition of thin metallic films bombarded by fast argon atoms. *Instrum. Exp. Technol.* **2014**, *57*, 345–351. [CrossRef]
46. Vereschaka, A.A.; Volosova, M.A.; Grigoriev, S.N.; Vereschaka, A.S. Development of wear-resistant complex for high-speed steel tool when using process of combined cathodic vacuum arc deposition. *Procedia CIRP* **2013**, *9*, 8–12. [CrossRef]
47. Metel, A.; Grigoriev, S.; Melnik, Y.; Panin, V.; Prudnikov, V. Cutting Tools Nitriding in Plasma Produced by a Fast Neutral Molecule Beam. *Jpn. J. Appl. Phys.* **2011**, *50*, 08JG04. [CrossRef]
48. Vereschaka, A.; Tabakov, V.; Grigoriev, S.; Sitnikov, N.; Milovich, F.; Andreev, N.; Bublikov, J. Investigation of wear mechanisms for the rake face of a cutting tool with a multilayer composite nanostructured Cr–CrN-(Ti,Cr,Al,Si)N coating in high-speed steel turning. *Wear* **2019**, *438*, 203069. [CrossRef]
49. Vereschaka, A.; Tabakov, V.; Grigoriev, S.; Sitnikov, N.; Milovich, F.; Andreev, N.; Sotova, C.; Kutina, N. Investigation of the influence of the thickness of nanolayers in wear-resistant layers of Ti-TiN-(Ti,Cr,Al)N coating on destruction in the cutting and wear of carbide cutting tools. *Surf. Coat. Technol.* **2020**, *385*, 125402. [CrossRef]
50. Evaristo, M.; Fernandes, F.; Jeynes, C.; Cavaleiro, A. The Influence of H Content on the Properties of a-C(W):H Coatings. *Coatings* **2023**, *13*, 92. [CrossRef]
51. Vereschaka, A.; Grigoriev, S.; Tabakov, V.; Migranov, M.; Sitnikov, N.; Milovich, F.; Andreev, N. Influence of the Nanostructure of Ti-TiN-(Ti,Al,Cr)N Multilayer Composite Coating on Tribological Properties and Cutting Tool Life. *Tribol. Int.* **2020**, *150*, 106388. [CrossRef]
52. Haq, A.J.; Munroe, P.R.; Hoffman, M.; Martin, P.J.; Bendavid, A. Berkovich indentation of diamondlike carbon coatings on silicon substrates. *J. Mater. Res.* **2008**, *23*, 1862–1869. [CrossRef]
53. Grigoriev, S.; Vereschaka, A.; Zelenkov, V.; Sitnikov, N.; Bublikov, J.; Milovich, F.; Andreev, N.; Mustafaev, E. Specific features of the structure and properties of arc-PVD coatings depending on the spatial arrangement of the sample in the chamber. *Vacuum* **2022**, *200*, 111047. [CrossRef]
54. Vereschaka, A.A.; Vereschaka, A.S.; Grigoriev, S.N.; Kirillov, A.K.; Khaustova, O.U. Development and research of environmentally friendly dry technological machining system with compensation of physical function of cutting fluids. *Procedia CIRP* **2013**, *7*, 311–316. [CrossRef]
55. Kyzioł, K.; Jabłoński, P.; Niemiec, W.; Prażuch, J.; Kottfer, D.; Łętocha, A.; Kaczmarek, Ł. Deposition, morphology and functional properties of layers based on DLC:Si and DLC:N on polyurethane. *Appl. Phys. A* **2020**, *126*, 751. [CrossRef]
56. Ahmed, S.F.; Mitra, M.K.; Chattopadhyay, K.K. Low-macroscopic field emission from siliconincorporated diamond-like carbon film synthesized by dc PECVD. *Appl. Surf. Sci.* **2007**, *253*, 5480–5484. [CrossRef]
57. Puttichaem, C.; Souza, G.P.; Ruthe, K.C.; Chainok, K. Characterization of Ultra-Thin Diamond-Like Carbon Films by SEM/EDX. *Coatings* **2021**, *11*, 729. [CrossRef]

58. Zeng, Q.; Ning, Z. High-temperature tribological properties of diamond-like carbon films: A review. *Rev. Adv. Mater. Sci.* **2021**, *60*, 276–292. [CrossRef]
59. He, M.; Yeo, C. Evaluation of Thermal Degradation of DLC Film Using a Novel Raman Spectroscopy Technique. *Coatings* **2018**, *8*, 143. [CrossRef]
60. Huang, B.; Liu, L.-T.; Han, S.; Du, H.-M.; Zhou, Q.; Zhang, E.-G. Effect of deposition temperature on the microstructure and tribological properties of Si-DLC coatings prepared by PECVD. *Diam. Relat. Mater.* **2022**, *129*, 109345. [CrossRef]
61. Moolsradoo, N.; Abe, S.; Watanabe, S. Thermal Stability and Tribological Performance of DLC-Si–O Films. *Adv. Mater. Sci. Eng.* **2011**, *2011*, 483437. [CrossRef]
62. Zeng, Q.; Eryilmaz, O.; Erdemir, A. Superlubricity of the DLC films-related friction system at elevated temperature. *RSC Adv.* **2015**, *5*, 93147–93154. [CrossRef]
63. Zajíčková, L.; Buršíková, V.; Peřina, V.; Macková, A.; Janča, J. Correlation between SiOx content and properties of DLC:SiOx films prepared by PECVD. *Surf. Coat. Technol.* **2003**, *174–175*, 281–285. [CrossRef]
64. Grischke, M.; Hieke, A.; Morgenweck, F.; Dimigen, H. Variation of the Wettability of DLC-coatings by NetworkModification Using Silicon and Oxygen. *Diam. Relat. Mater.* **1998**, *7*, 454–458. [CrossRef]
65. Meškinis, Š.; Vasiliauskas, A.; Andrulevičius, M.; Peckus, D.; Tamulevičius, S.; Viskontas, K. Diamond Like Carbon Films Containing Si: Structure and Nonlinear Optical Properties. *Materials* **2020**, *13*, 1003. [CrossRef]
66. Maser, K. Varying internal parameters in the thermal silicon oxidation. *J. Solid State Electrochem.* **2019**, *23*, 2589–2593. [CrossRef]
67. Gerlach, G.; Maser, K. A Self-Consistent Model for Thermal Oxidation of Silicon at Low Oxide Thickness. *Adv. Condens. Matter Phys.* **2016**, *2016*, 7545632. [CrossRef]
68. Hatty, V.; Kahn, H.; Heuer, A.H. Fracture Toughness, Fracture Strength, and Stress Corrosion Cracking of Silicon Dioxide Thin Films. *J. Microelectromech. Syst.* **2008**, *17*, 943–947. [CrossRef]
69. Zarchi, M.; Ahangarani, S. Optical and morphological properties of silicon dioxide thin films. *J. Mater. Sci: Mater. Electron.* **2016**, *27*, 1165–1170. [CrossRef]
70. Jeong, J.S.; Cho, C.H.; Kim, J.O.; Yeo, D.H.; Choi, W.Y. Preparation and characterization of DLC/SiO_2/Al_2O_3 nanofiltration membrane. *Bull. Mater. Sci.* **2013**, *36*, 1133–1138. [CrossRef]
71. Grigoriev, S.; Vereschaka, A.; Milovich, F.; Tabakov, V.; Sitnikov, N.; Andreev, N.; Sviridova, T.; Bublikov, J. Investigation of multicomponent nanolayer coatings based on nitrides of Cr, Mo, Zr, Nb, and Al. *Surf. Coat. Technol.* **2020**, *401*, 126258. [CrossRef]
72. Vetter, J.; Eriksson, A.O.; Reiter, A.; Derflinger, V.; Kalss, W. Quo Vadis: AlCr-Based Coatings in Industrial Applications. *Coatings* **2021**, *11*, 344. [CrossRef]